Active Matter: from motility to self-organization
Lectures presented at the Boulder School on *Self-Organizing Matter* July 2024

M. Cristina Marchetti[1]

[1] *Department of Physics, University of California Santa Barbara, Santa Barbara, CA 93106, USA*

CONTENTS

I. INTRODUCTION

The name active matter refers to collections of entities that individually consume free energy to generate motion and forces [1, 2]. Through interactions, these "active particles" (e.g., bacteria, phoretic colloids) spontaneously organize in emergent large-scale structures with a rich range of materials properties. The defining property of an active system is that the energy input that maintains the system out of equilibrium, whether truly internal or created by contact with a proximate surface, acts individually and independently on each active particle.

A few remarks:

- Once the chemo-mechanical processes that convert fuel into motion are integrated out, the dynamics of active particles breaks time reversal symmetry (TRS) in a local and sustained manner.

- The TRS-breaking of active systems should be contrasted with more conventional nonequilibrium systems that are displaced from equilibrium globally by an external force that picks out a direction in space, such as an electric field, or as in sedimentation under gravity, or are forced at the boundaries, such as through an imposed mechanical shear.

- Due to the breaking of TRS at the microscale, active systems do not obey detailed balance and can generate self-sustained flows and cyclical currents. Thus, steady-state movies of active dynamics run forwards and backwards do not look the same, as they would in Newtonian mechanics.

- In contrast to the dynamics of, say, sedimenting particles, the dynamics of active particles is "force free".

- Nonreciprocal interactions that evade Newton's Third Law of action-reaction are ubiquitous in active and living systems that break detailed balance at the microscale, from social forces to promoter-inhibitor couplings among cell types in developing organs and organisms, to antagonistic interspecies interactions in bacteria and prey-predator systems .

There are at this point many reviews focusing on different aspects of active matter [3–6], a few books, and even a "review of reviews" that classifies various review articles [7].

I would like to add a warning: this set of notes is a bit of a one side view of a very broad field of rapidly evolving research, and does not contains a complete and historically accurate set of citations. For a complete set of citations, please consult suitable review articles.

A. Examples of active systems

For concreteness, let us consider a specific example: bacteria. For instance, *E.coli* is a rod-shaped bacterium with a body about $2-3\mu m$ long and $0.5\mu m$ in diameter and a long tail of flagella that allows it to swim [8]. It composes about 1% of the gut flora.

- An individual *E. Coli* swims through run-and-tumble: It travels in a straight line at a speed of $10-30\mu m/s$ and every second or so it spreads out its flagella and undergoes a tumble, i.e., a large change in direction [9]. Although we will see below that the dynamics is diffusive at times large compared to the tumble rate, this is not a conventional Random Walk.

- A dense *E. Coli* suspension exhibits coordinated motion and spontaneous organization at large scales:
  - It behaves like a self-flowing fluid: in a nutrient-rich medium one observes a characteristic swarming dynamics named bacterial turbulence.
  - When starved, *E.Coli* self-organizes in a variety of patterns, such concentric rings of high and low bacterial density or regular arrays of spots of high cell density.
  - It can form solid-like biofilms.

There are many many other examples spanning a broad range of scales, including:

- Organization of chromatin inside the cell nucleus
- Inside a cell (e.g., cytoskeleton controlling cell division, motility)
- Many cells: biological tissue, wound healing, development
- Insect, fish, bird, people
- Collections of robots
- Phoretic colloids, engineered microswimmers
- Reconstituted suspensions of motor proteins (myosins, kinesins) and cytoskelatal filaments (F-actin, microtubules).

B. Classes of active matter

Active systems spontaneous organize in a variety of collective phases with properties and behavior controlled by the symmetry of both the active "particles" and their interactions. Four important classes are [2, 6]:

- *Scalar active matter.* Spherical active particles (e.g., colloids driven by a variety of phoretic effects) with radially symmetric interactions and no alignment can undergo motility induced phase separation (MIPS) even in the absence of any attractive interactions. This is called scalar active matter because the order parameter that describes the transition is the density difference between the dilute and the dense phases, hence a scalar. A local number density field can be generally defined as

$$\rho(\mathbf{r},t) = \Big\langle \sum_n \delta(\mathbf{r}-\mathbf{r}_n(t)\Big\rangle \,, \tag{1}$$

  where $\mathbf{r}_n$ is the position of the n-th particle.

- *Polar active matter.* Active particles with a head and a tail, such as many bacteria, birds or fish, are polar and can organize in states with polar order quantified by a vectorial order parameter. This can be defined as a polarization density field in terms of unit vectors $\boldsymbol{\nu}_n$ identifying the polarization of each unit ,

$$\mathbf{p}(\mathbf{r},t) = \Big\langle \sum_n \boldsymbol{\nu}_n \delta(\mathbf{r}-\mathbf{r}_n(t)\Big\rangle \,, \tag{2}$$

  where the brackets denote an average over the system. An example is flocking agents where the polarization (up to a factor of propulsive speed) is also is the mean velocity of the flock. Polar active particles can also antialign, in which case they may organize in a state with nematic (apolar) order.

- *Nematic active matter* Apolar active particles have no head and tail and exert force dipoles on their surroundings. Examples are microtubule-kinesin bundles or melanocytes, the cells that shake the pigment in our skin. They can organize in states with nematic order, which is quantified by a tensorial order parameter, defined as (see below for explanation)

$$Q_{ij}(\mathbf{r},t) = \frac{1}{\rho}\Big\langle \sum_n \left(\nu_{ni}\nu_{nj} - \frac{1}{d}\delta_{ij}\right)\delta(\mathbf{r}-\mathbf{r}_n(t)\Big\rangle \,, \tag{3}$$

  where d is the dimensionality of the system. Here and below $i, j, k, ...$ are used for Carthesian components.

- *Chiral active matter.* Active particles may be chiral and organize in states with microscopic chirality. An example are colloidal spinners in a fluid. In two dimensions, chirality is captured by a psuedoscalar that quantifies the rotation frequency and can be deifned as

$$\Omega(\mathbf{r},t) = \Big\langle \sum_n \Omega_n \delta(\mathbf{r}-\mathbf{r}_n(t)\Big\rangle \,, \tag{4}$$

  wher Ω_n is the spinning rate of particle n.

This is not an exhaustive list. For instance, it is of course possible to have chiral polar and chiral nematic states, as well as active solids that can exhibit translational order.

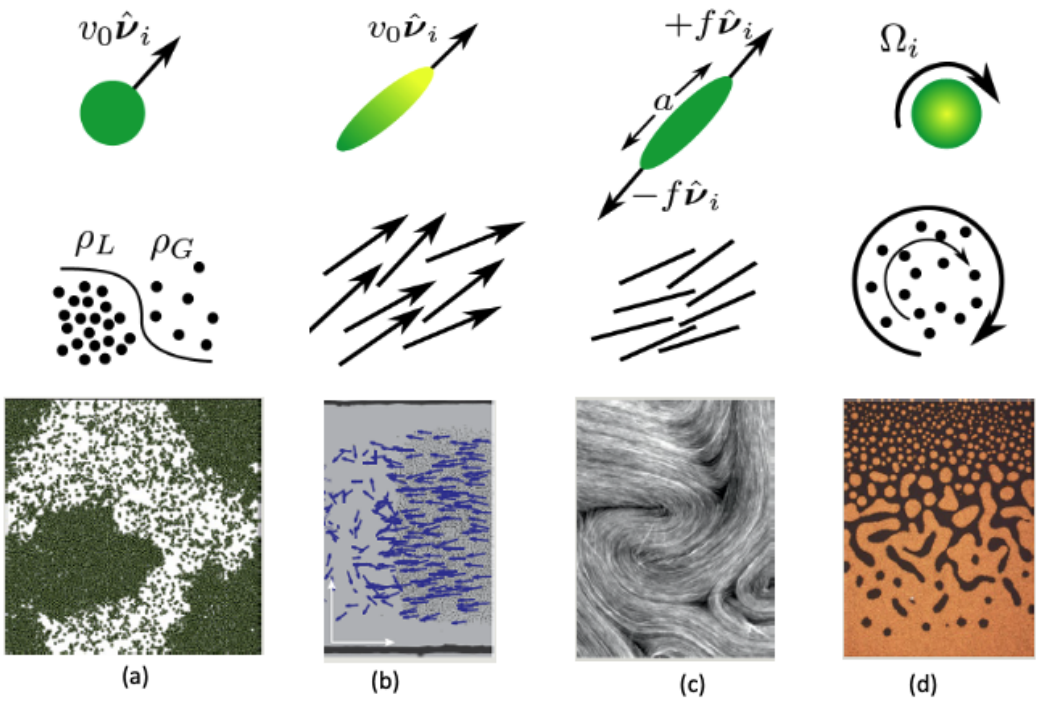

Figure 1. Various classes of active matter. (a) Scalar active matter composed of isotropic particles self-propelled at speed v_0 along an axis $\hat{\boldsymbol{\nu}}_i$ that undergo MIPS. (b) Polar active matter composed of selfpropelled polar aligning active particles that undergo a flocking transition. (c) Nematic active matter of eleongated particles that extert force dipoles on their environment. (d) Chiral active matter composed of particles that self-spin at a rate Ω_i in two dimensions. The images in the bottom row are, from right to left: MIPS in a fluid of active Brownian particles (adapted from Ref. [10]); a flock of colloidal polar particles (adapted from Ref. [11]); a microtubule-kinesin active nematic (adapted from Ref. [12]); a fluid of colloidal spinners (adapted from Ref. [13]).

C. A bit of history of the field

In 1995 the Hungarian physicist Tamás Vicsek proposed a minimal model of bird flocking inspired by the physics of magnetism [14]. He showed that a collection of flying spins - self-propelled point particles traveling with fixed speed in a direction updated by alignment with neighbors in a noisy environment - can undergo a phase transition from a disordered state where the spins fly randomly in all directions to an ordered state of collective motion. Just a few months later, Vicsek presented his work in a seminar at IBM Yorktown Heights. John Toner and Yuhai Tu realized that they could turn Vicsek's agent-based model into a field theory and formulated what are now known as the Toner-Tu equations of flocking [15].

Truth be told, what physicists now know as the Vicsek model had effectively been previously formulated by Craig Reynolds, a computer scientist working for the animation industry, who in 1986 created *Boids* [16] – an agent-based simulation of collective motion that he employed, for instance, to generate the animation of flying bats in the 1992 feature *Batman Returns*. Indeed the

model appears even earlier in the literature, in theories of fish schools by Aoki [17] and Partridge [18]. While these contributions remained unnoticed by the physics community for some years, Reynolds, a leader in the development of three-dimensional animation, was awarded a Scientific and Technical Award by the Academy of Motion Picture Arts and Sciences in 1998. In the intervening years, the notion introduced by Vicsek that the collective dynamics of self-driven entities can be described as a nonequilibrium phase transition gained enormous popularity among physicists and was shown to provide a powerful framework for describing spontaneous organization on many scales. For their key contribution to the creation of the field of active matter, Vicsek, Toner and Tu received the Lars Onsager prize of the American Physical Society in 2020.

The first published use of the term Active Matter appears to be in Ref. [19]. Active Membranes appear a little earlier in the physics literature [20, 21]. The term "active" in reference to fuel-driven transport across a membrane, against a concentration gradient, is standard in biology [22]. Active stresses in a fluid medium suffused with sustained energy conversion make their first appearance in Ref [23].

II. ACTIVE DYNAMICS VERSUS BROWNIAN DYNAMICS

To understand the key role of motility in driving self-organization, it is useful to begin by contrasting the dynamics of an active or self-propelled particle to that of a familiar Brownian particle. At least three types of active dynamnics are commonly considered in the literature: Active Brownian Particles (ABPs), Active Ornstein-Uhlenbeck Particles (AOUPs), and Run-and-Tumble Particles (RTP). Here we will mainly focus on ABPs and briefly mention the connection to this other commonly considered dynamics. A comprehensive review can be found in Ref. [3].

A. Brownian motion

Let us start with a brief summary of how we describe Brownian motion - the herratic motion of a colloidal particle of mass m in a fluid in thermal equilibrium at temperature T. An excellent description of Brownian morion can be found in Ref. [24]. We write a stochastic equation of motion or Langevin equation for the velocity $\mathbf{v}$ of the particle as

$$m\frac{d\mathbf{v}}{dt} = -\gamma\mathbf{v} + \mathbf{f}(t) \; . \tag{5}$$

The right hand side of Eq. (5) represents the forces due to the fluid. The first term is the mean drag from the surrounding fluid. The second term represents the random kicks that the colloid receives from collisions with fluid molecules that drives the motion of the Brownian particle. The effect of such collisions is modeled as a stochastic force with Gaussian distribution and zero mean, i.e.,

$$\begin{aligned} \langle \mathbf{f}(t) \rangle &= 0 \; , \\ \langle f_i(t) f_j(t') \rangle &= 2\Delta\delta_{ij}\delta(t-t') \; , \end{aligned} \tag{6}$$

where i, j denote Carthesian components and the variance Δ will be determined by requiring the Brownian particle to be in thermal equilibrium with the fluid at long times. The $\delta(t)$ correlations of the random forces corresponds to the assumption that successive kicks/collisions are uncorrelated in time. Note that this equation contains a characteristic time scale $\tau = m/\gamma$ that represents the relaxation time of the mean velocity, $\langle \mathbf{v}(t) \rangle = \mathbf{v}(0)e^{-t/\tau}$. Importantly, here the equilbrium ambient

fluid generates both the dissipation and the drive. Since we have in mind a micron-size colloid, the drag or friction coefficient γ can be calculated in the low Reynold number limit. For a spherical particle of radius R in $3D$ it is given by the Stokes expression $\gamma = 6\pi\eta R$, where η is the shear viscosity of the fluid.

To determine Δ, we formally integrate Eq. (5). Assuming for simplicity $\mathbf{v}(0) = 0$, we find

$$\mathbf{v}(t) = \frac{1}{m}\int_0^t dt' e^{-(t-t')/\tau}\mathbf{f}(t') \ . \tag{7}$$

It is then easy to show that

$$\langle|\mathbf{v}(t)|^2\rangle = \frac{\Delta}{m\gamma}d\left(1 - e^{-2t/\tau}\right) \ . \tag{8}$$

We require that at long time ($t \gg \tau$) the Brownian partcile be in thermal equilibrium with the fluid. This means that $\langle|\mathbf{v}(t\to\infty)|^2\rangle$ must be the equilibrium value from equipartition $\langle|\mathbf{v}(t)|^2\rangle_{eq} = d\frac{k_BT}{m}$. This gives

$$\Delta = \gamma k_B T \ . \tag{9}$$

The dynamics of Brownian particles is generally quantified in terms of the Mean-Square Displacement (MSD). This is easily obtained from the Langevin equation as

$$\langle[\mathbf{r}(t) - \mathbf{r}(0)]^2\rangle = 2d\frac{k_BT}{\gamma}\left[t - \tau\left(1 - e^{-|t|/\tau}\right)\right] \ . \tag{10}$$

It is useful to consider two limiting cases of this expression. Letting $\Delta\mathbf{r} = \mathbf{r}(t) - \mathbf{r}(0)$, we find

$$\langle[\Delta\mathbf{r}]^2\rangle = \begin{cases} d\frac{k_BT}{m}t^2 & \text{for} \quad t \ll \tau \quad \text{ballistic} \\ \\ 2dDt & \text{for} \quad t \gg \tau \quad \text{diffusive} \end{cases} \tag{11}$$

where

$$D = \lim_{t\to\infty}\frac{\langle[\Delta\mathbf{r}(t)]^2\rangle}{2dt} = \frac{k_BT}{\gamma} \tag{12}$$

is the diffusion coefficient. Equation (12) is known as the Einstein relation and is the simplest example of fluctuation-dissipation theorem (FDT). It also provides a useful metric for quantifying the rheological state of a system. By inserting the Stokes expresison for the drag γ we obtain $D = \frac{k_BT}{6\pi\eta R}$ which is known as the Stkes-Einstein relation.

Problem 1: Green-Kubo formula

Show that the diffusion coefficient can also be written as

$$D = \frac{1}{d}\int_0^\infty dt\langle\mathbf{v}(t)\cdot\mathbf{v}(0)\rangle \ . \tag{13}$$

This is the simplest example of a Green-Kubo formula that expresses a transport coefficient in term of an equilibrium time correlation function.

Note that if we consider from the outset the overdamped limit where $t \gg \tau$, we can neglect inertia in Eq. (5), which reduces to

$$\gamma\frac{d\mathbf{r}}{dt} = \mathbf{f}(t) \ . \tag{14}$$

In this limit the MSD is always diffusive, with

$$\langle [\Delta \mathbf{r}]^2 \rangle = 2dDt \ . \tag{15}$$

Finally, an equivalent description of Brownian motion (or in general stochastic dynamics) is in terms of the probability distribution $P(\mathbf{r}, \mathbf{v}, t)$ of finding the particle in a neighborhood $(d\mathbf{r}, d\mathbf{v})$ of $(\mathbf{r}, \mathbf{v})$ at time t. One can show that the probability distribution of a particle with dynamics described by Eq. (5) is described by a Fokker-Planck equation [24]. Here we are mainly interested in situation where the velocity relaxes very quickly and the dynamics is overdamped. For this reason we will simply consider the distribution $P(\mathbf{r}, t)$ of particles' positions. For concreteness, it is, however useful to consider the case of an overdamped particle subject to a force $\mathbf{F}_e = -\boldsymbol{\nabla} V_e$. The Langeving equation is then given by

$$\gamma \frac{d\mathbf{r}}{dt} = \mathbf{F}_e + \mathbf{f}(t) \ . \tag{16}$$

One can then show that the probability distribution of positions satisfies the following Fokker-Planck equation (usually referred to as Smoluchowski equation in the overdamped limit)

$$\partial_t P(\mathbf{r}, t) = -\frac{1}{\gamma} \boldsymbol{\nabla} \cdot (\mathbf{F}_e P) + D \nabla^2 P \ . \tag{17}$$

B. A single Active Brownian Particle

A minimal models of an active or self-propelled particle is obtained by adding to the particle's dynamics a sustained energy source that embodies the microscopic conversion of energy stored in the environment into directed motion. The resulting propulsion force is subject to fluctuations which are generally not thermal in origin. For simplicity, we neglect inertial effects and restrict ourselves to particles in $2D$. An ABP is then described by the position $\mathbf{r}$ of its center of mass and a unit vector $\boldsymbol{\nu} = (\cos\theta, \sin\theta)$ that denotes the direction of self-propulsion. The translational dynamics is governed by the balance of propulsion, possibly an external potential U, and noise, and is described by the Langevin equation given by

$$\gamma \dot{\mathbf{r}} = f_0 \boldsymbol{\nu} - \boldsymbol{\nabla} U + (2D)^{1/2} \boldsymbol{\eta}(t) \ , \tag{18}$$

where f_0 denotes the propulsive force and $v_0 = f_0/\gamma$ is the propulsion speed, assumed constant. Here $D = k_B T/\gamma$ is the thermal translational diffusion coefficient introduced earlier. Since the variance of thermal noise has been scaled out, the stochastic force $\boldsymbol{\eta}(t)$ is Gaussian distributed with zero mean and unit variance, $\langle \boldsymbol{\eta}(t) \rangle = 0$ and $\langle \eta_i(t) \eta_j(t') \rangle = \delta_{ij} \delta(t - t')$. The direction of the propulsive force changes stochastically according to

$$\dot{\theta} = \sqrt{2D_R} \ \eta_R(t) \tag{19}$$

where D_R is a rotational diffusion coefficient and $\eta_R(t)$ a Gaussian random force with zero mean and unit variance.

This model captures the directionality of the self-propulsion, namely the ability of the orientation to stay constant during a typical persistence time $\tau_p = D_R^{-1}$ and corresponds to an exponential decay in time of the correlations of the polarity $\boldsymbol{\nu}$,

$$\big\langle \nu_i(t) \nu_j(0) \big\rangle = \delta_{ij} \frac{v_0^2}{d} e^{-|t|/\tau} \ . \tag{20}$$

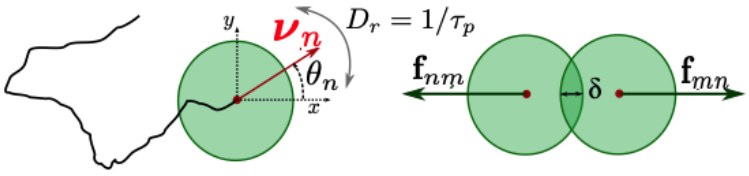

Figure 2. Sketch of an Active Brownian Particle (left) and two particles repelled by soft forces upon overlapping a distance δ.

In other words, an ABP can also be thought of as a Brownian particle with colored noise, in addition to δ-correlated thermal noise. Of course colored noise alone would not break detailed balance as the fluctuation-dissipation theorem (FDT) would still hold if the friction were chose to be nonlocal in time. What breaks detailed balance and FDT in this minimal model is the fact that the friction is constant, while the effective noise is correlated in time.

The MSD of a single ABP is given by

$$\left\langle \Delta \mathbf{r}^2(t) \right\rangle = 2d\left(D + D_{\rm sp}\right)|t| + 2(v_0\tau)^2\left(e^{-|t|/\tau} - 1\right) = \begin{cases} 2dD\,|t| + v_0^2 t^2 & \text{for } t \ll \tau_p, \\ 2d\left(D_{\rm t} + D_{\rm sp}\right)|t| & \text{for } t \gg \tau_p. \end{cases} \tag{21}$$

with $D_{sp} = v_0^2\tau_p/d$. For a micron-size colloid suspended in water at ambient temperature, the translational diffusion coefficient is of the order of $D_{\simeq}0.1\,\mu\mathrm{m}^2/\mathrm{s}^{-1}$, whereas the active diffusion coefficient of self-phoretic colloids is of the order of $D_{\rm sp} \simeq 10^2\,\mu\mathrm{m}^2/\mathrm{s}^{-1}$. For this reason in the following we will neglect thermal translational diffusion.

The ABP exhibits ballistic dynamics for $t \ll \tau_p$ and diffusive dynamics for $t \gg \tau_p$. Therefore, the dynamics of an isolated self-propelled particle at times and distances larger than, respectively, the persistence time τ_p and the persistence length $\ell_p = v_0\tau_p$ can not be distinguished from a "hot" Brownian Particle at temperature $T_{eff} = \gamma D_{\rm sp}$).

ABPs were introduced to mimick the dynamics of self-phoretic colloids with asymmetric chemical and/or physical properties [25, 26]. Other models of self-propulsion have been considered that differ by the assumptions made on the higher order cumulants of the noise statistics. Here we just briefly describe two other models. The run-and-tumble motion is inspired by the dynamics of bacteria [27, 28]. It alternates between an active state when the particles moves at constant speed v_0 in a given direction ("run"), and a passive state when the center of mass of the particle stays constant while reorienting its direction ("tumble"). In practice, the change of direction is taken as instantaneous and completely isotropic, occurring with a given rate α, so that typical trajectories are made of straight lines with random length of typical size v_0/α.

The dynamics of AOUPs was originally proposed as an approximated treatment of ABPs [29, 30]. It consists in neglecting the non-Gaussian nature of the self-propulsion statistics, which amounts to allowing the amplitude of self-propulsion to fluctuate. In practice, such an approximation captures the emergent behavior of ABPs with a better accuracy in three dimensions than two. The self-propulsion dynamics can be described as an Ornstein-Uhlenbeck process

$$\tau_p\dot{\boldsymbol{\nu}} = -\boldsymbol{\nu} + (2D_{\rm sp})^{1/2}\boldsymbol{\chi}, \tag{22}$$

where $\boldsymbol{\chi}$ is a Gaussian noise with correlations $\langle \chi_\alpha(t)\chi_\beta(0)\rangle = \delta_{\alpha\beta}\delta(t)$ completely uncorrelated with $\boldsymbol{\eta}$. Comparing this to the dynamics of an underdamped passive Brownian particle, we see that the effect of the noise persistence amounts to introducing (i) an effective inertia controlled by the persistence time τ_p and (ii) a velocity-dependent mobility. Moreover, in the limit of vanishing persistence at fixed $D_{\rm sp}$ the original dynamics given in Eq. (18) reduces to the one of an overdamped passive Brownian particle at a temperature $\gamma(D+D_{\rm sp})$. Therefore, the persistence can be regarded as the only parameter monitoring the nonequilibrium properties of an AOUP [31].

The MSD has the same form for the three models of self-propulsion presented above, since it only depends on the two-point correlations of the fluctuations.

Problem 2: MSD of a single Active Brownian Particle.
Consider a single APB with dynamics described by the equations

$$\partial_t \mathbf{r} = v_0 \boldsymbol{\nu} + \sqrt{2D}\ \boldsymbol{\eta}\ ,$$
$$\partial_t \theta = \sqrt{2D_R}\ \eta_R\ ,$$

where $\mathbf{r}$ is the center of mass of the particle. The ABP moves with a speed v_0 along a unit vector $\boldsymbol{\nu} = \cos\theta\hat{\mathbf{x}} + \sin\theta\hat{\mathbf{y}}$ that is pinned to its body axis. The self propulsion is not perfect in that it meanders a bit. This is captured by the θ equation where η_R is a stochastic white noise that causes the direction to fluctuate. $\boldsymbol{\eta}$ is the translational white noise that gives rise to diffusion. The noise has zero mean and correlations

$$\langle \eta_i = (t)\, \eta_j\,(t')\rangle = \delta_{ij}\delta\,(t-t')$$
$$\langle \eta_R\,(t)\, \eta_R\,(t')\rangle = \delta\,(t-t')$$

and all higher cumulants are zero, i.e., the noise is Gaussian. Our goal is to compute the MSD of the partcile, i.e., derive Eq. (21) of the notes.$\langle r_\alpha\,(t)\, r_\beta\,(t)\rangle$.

1. Show that

$$\langle \boldsymbol{\nu}\,(t)\, \boldsymbol{\nu}\,(t')\rangle = \frac{1}{2}\begin{pmatrix} \cos 2\theta_0 \exp\left(-D_R\left[t+t'+2\min\left(t,t'\right)\right]\right) & \sin 2\theta_0 \exp\left(-D_R\left[t+t'+2\min\left(t,t'\right)\right]\right) \\ +\exp\left(-D_R\left[t+t'-2\min\left(t,t'\right)\right]\right) & -\cos 2\theta_0 \exp\left(-D_R\left[t+t'+2\min\left(t,t'\right)\right]\right) \\ \sin 2\theta_0 \exp\left(-D_R\left[t+t'+2\min\left(t,t'\right)\right]\right) & +\exp\left(-D_R\left[t+t'-2\min\left(t,t'\right)\right]\right) \end{pmatrix}$$

2. Now compute $\langle r_i\,(t)\, r_j\,(t)\rangle$ (assume $\mathbf{r}(t=0)=0$). You can average over the initial angle θ_0.

3. Now analyze the form of the mean square displacement at short times i.e., $t << \frac{1}{D_R}$ and at long times, i.e., $t >> \frac{1}{D_R}$.

4. Write a program to evaluate numerically the MSD of a single APB neglecting the translational noise and compare your numerical result to your calculation, as well as to the MSD of a single overdamed Brownian particle.

5. Define an effective temperature T_{eff} for your ABP. Research the literature to find suitable parameters for, say, a typical Janus active colloid and evaluate T_{eff}.

C. Adding Interactions

Interactions are of course essential for self-organization. We can classify the type of interactions that have been considered as follows:

- steric interactions: play a key role in driving MIPS and active jamming, but also nematic order if the particles are rod-like;
- aligning interactions: can be polar or apolar in nature, driving flocking or active nematic states;
- shape-based interactions, as in Vertex and Voronoi models used to describe confluent epithelial tissues, which are topological in nature;
- quorum sensing, where microbes interact by secreting some chemical molecules to which other cells respond, or react to the density of their neighbors.

Here we will focus on the first two.

Once interactions are present, it is of course much harder to construct theories capable of predicting the behavior of the system. Most common tools are:

- numerical simulations, either agent-based or particle models;
- continuum theories.

Here we will focus on continuum theories. So let me tell you a bit more about how these can be constructed.

a. How to construct a continuum theory. Often the complexity of the dynamics, inherent to the large number of degrees of freedom, can be reduced by using a continuum description of the system at large scales in terms of a small number of coarse-grained fields. The resulting description is an effective field theory often referred to as hydrodynamics. The first step in constructing a hydrodynamic theory is identifying the fields. To do this, we rely on the notion of separation of time scales: most fluctuations decay on microscopic, short time scales; some, however, are "slow", in the sense that fluctuations of wavelength $\sim 2\pi/q$ decay at a rate $s(q)$ that vanishes when $q \to 0$. A familiar example is diffusion that describes how a local density inhomogeneity or fluctuation $\delta\rho$ decays to eventually reach a state of homogeneous density. This dynamics is governed by the diffusion equation

$$\partial_t \delta\rho = D\nabla^2 \delta\rho \,, \tag{23}$$

where D is the diffusion coefficient. The $\mathbf{q}-$Fourier amplitude of a density fluctuation then decays as $\delta\rho_{\mathbf{q}}(t) \sim e^{-Dq^2 t}$. The decay rate $s(q) = -Dq^2$ vanishes at large wavelength because density is a conserved field ($\int d\mathbf{r}\rho = N$, with N the number of particles in the system) and fluctuations can only decay through material being rearranged from one location to another.

In general, hydrodynamic fields, defined as those whose relaxation rate vanishes when $q \to 0$, are those associated with (i) conservation laws and (ii)spontaneous broken symmetries. If we wish to describe a phase transition, however (as opposed to just the properties of an ordered state), we often include in continuum models the full order parameter even if its magnitude is not strictly a hydrodynamic mode.

Once the relevant fields are identified, the corresponding continuum theory can then be constructed from four different routes:

1. based on phenomenological arguments, such as the symmetries of the system [15, 32];

2. by introducing constitutive equations between the fluxes and the forces identified from the entropy production rate close to equilibrium [33, 34];

3. via explicit coarse-graining of the microscopic dynamics [35–37]. The latter provides explicit expressions for the kinetic coefficients appearing in the theory, whereas such coefficients are unknown *a priori* from the two other methods. Yet, the coarse-graining procedures generally need to be combined with some approximations (e.g., low density, weak interactions) to arrive at some closed form for the dynamical equations.

4. Recently the combination of (i) high resolution imaging that has made available large amount of detailed data, and (ii) machine learning aproaches and data-driven algorythims has provided a new path for learning continuum models from data [38, 39].

Here I will generally just introduce the continuum models with no derivation, but with some justification.

Finally, we should keep in mind that biological systems may be guided by completely different rules, such as the need to optimize information transmission, evolution and survival of the fittest, the development of structures designed to perform specific functions. The notions of broken symmetries and conservation laws inspired by condensed matter physics are very useful, but we must to keep a fresh and open mind in the search for new principles that may govern biology.

III. SCALAR ACTIVE MATTER: MOTILITY INDUCED PHASE SEPARATION (MIPS)

The name scalar active matter is used to describe systems of isotropic motile particles with radially symmetric interactions. The simplest case is when the interactions are purely repulsive. Even in this simple case, motility can have profound effects on the collective behavior, driving two nonequilibrium phase transitions:

- MIPS: a type of liquid-gas condensation that occurs in the absence of any attractive interactions [10, 25, 26, 28, 40];

- glassy/jammed states at high density, with dynamical heterogeneities and behavior typical of glassed, observed for instance in confluent biological tissue [41–44].

In this lectures I will focus on MIPS. If you are intersted in active jamming, there are some excellent reviews, such as Refs. [42, 44].

To examine the remarkable behavior of a minimal model with just motility and purely isotropic steric interactions, we consider a collection of N disc-shaped ABPs in two dimensions interacting with pairwise repulsive forces. Interactions, even just steric ones, reveal the nonequilibrium nature of ABPs and how motility alone can engender self-organization not possible in equilibrium.

The microscale dynamics is governed by a set of coupled Langevin equations, given by

$$\dot{\mathbf{r}}_n = v_0 \boldsymbol{\nu}(\theta_n) + \frac{1}{\gamma} \sum_{m \neq n} \mathbf{f}_{nm} \,, \tag{24}$$

$$\dot{\theta}_n = \sqrt{2D_{\mathrm{R}}}\, \eta_n, \tag{25}$$

where η_n are uncorrelated Gaussian noises with zero mean and correlations

$$\left\langle \eta_n(t)\eta_m(0)\right\rangle = \delta_{nm}\delta(t). \tag{26}$$

and we have neglected translational thermal noise. The forces $\boldsymbol{f}_{nm} = -\nabla_n V(\mathbf{r}_m - \mathbf{r}_n)$, with $V(\mathbf{r}_n - \mathbf{r}_m)$ the pair potential, are purely repulsive. The results described below do not qualitatively depend on the specific form chosen for the interaction potential. A common form used in the literature are soft repulsive forces $\boldsymbol{f}_{nm} = f_{nm}\hat{\boldsymbol{r}}_{nm}$, with $\hat{\boldsymbol{r}}_{nm} = (\boldsymbol{r}_n - \boldsymbol{r}_m)/r_{nm}$, $r_{nm} = |\boldsymbol{r}_n - \boldsymbol{r}_m|$, and $f_{nm} = k(a_n + a_m - r_{nm})$ if $r_{nm} < a_n + a_m$ and $f_{nm} = 0$ otherwise. Here a_n is the radius of the n-partcile. For monodisperse systems $a_n = a$ independent of n.

Useful dimensionless parameter to describe N ABPs in a $2D$ area A are the packing fraction $\phi = \sum_n \pi a_n^2/A$ and the rotational Péclet number defined as the ratio of the particle persistence length, $\ell_p = v_0\tau_p$, to its size a as $Pe = \ell_p/a$. Numerical simulations of this model show that repulsive ABPs phase separate into a dilute and a dense phase. This is surprising because in equilibrium phase separation requires attractive interactions. For monodisperse particles the dense phase can be hexatic or even crystalline. For polydisperse particles it is glassy. An example of the phase diagram for monodisperse discs from Ref. [45] is shown in Fig. 3.

The transition occurs because crowding slows down the particles' motility, and particles in turn accumulate where they show down, resulting in a runaway effect that leads to a spinodal instability or "antidiffusion". More precisely one can carry out a perturbative (in the density ρ of ABPs) calculation of the effect of interactions on the propulsive speed and show that, to leading order, $v_0 \to v(\rho) = v_0 + \mu\langle \boldsymbol{\nu}_n \cdot \sum_{m\neq n} \mathbf{f}_{nm}\rangle \simeq v_0(1 - \lambda\rho)$, with $\lambda > 0$. The phase separation can also be understood via a nice kinetic argument due to Redner *et al.* [26] that clearly shows that the persistent dynamics of ABPs breaks detailed balance: the flux of particles into a cluster ($J_{in} \sim \rho_{gas} v_0$) is different from the flux out of the cluster, which is controlled by the rate at which particles turn their nose outward ($J_{out} \sim (\tau_p a)^{-1}$). A simple estimate for phase separation is then given by $J_{in} \sim J_{out}$, which gives $\phi \sim Pe^{-1}$. This also corresponds to the statement that $\tau_p > \tau_{mf}$, with $\tau_{mf} \sim (2av_0\rho)^{-1}$ the mean free time between collisions. In other words, aggregation occurs when colliding particles do not have time to turn their nose away before experiencing more collisions.

The key simplifying feature of this model is that particles do not exert torques on each other nor on the surrounding medium. The angular dynamics of each particle is unaffected by that of the others and by interactions. In fact, as shown at the single particle level, the angular dynamics can be eliminated at the cost of turning the noise in Eq. (24) into colored noise, correlated over a perisistence time $\tau_p = D_R^{-1}$. It is then evident that the model breaks detailed balance in a minimal way because the constant mobility is not balanced by the colored noise.

A. Mean-Field-Theory of MIPS

To construct a simple Mean-Field-Theory of MIPS, we use Eq. (17) to write down the Smoluchowski equation for the probability distribution $\mathcal{P}(\mathbf{r}, \boldsymbol{\nu}, t)$ for an active particle to be at $\mathbf{r}$ with orientation $\boldsymbol{\nu}$ at time t

$$\partial_t \mathcal{P} = -\boldsymbol{\nabla} \cdot (v_0 \boldsymbol{\nu} \mathcal{P}) + D_R \partial_\theta^2 \mathcal{P} \tag{27}$$

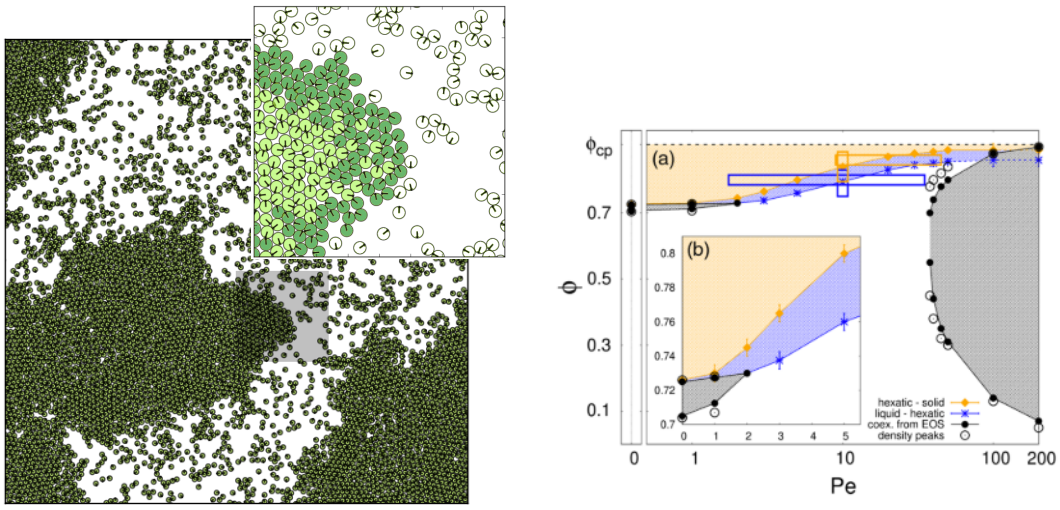

Figure 3. Left: Snapshot from simulations of MIPS. Right: Phase diagram of monodisperse ABPs in the plane of Péclet number Pe and packing fraction ϕ showing the coexistence region (gray), hexatic liquid (purple) and hexatic solid (yellows) regions (from Ref. [45].

The angular moments of $P(\mathbf{r}, \boldsymbol{\nu}, t)$ describe the local properties of ABPs as follows

$$\rho(\mathbf{r}, t) = \int d\boldsymbol{\nu}\ \mathcal{P}(\mathbf{r}, \boldsymbol{\nu}, t) \quad \text{density} \tag{28}$$

$$\mathbf{p}(\mathbf{r}, t) = \int d\boldsymbol{\nu}\ \boldsymbol{\nu}\ \mathcal{P}(\mathbf{r}, \boldsymbol{\nu}, t) \quad \text{polarization density} \tag{29}$$

$$\rho(\mathbf{r}, t) Q_{ij}(\mathbf{r}, t) = \int d\boldsymbol{\nu} \left(\nu_i \nu_j - \frac{1}{d} \delta_{ij} \right) \mathcal{P}(\mathbf{r}, \boldsymbol{\nu}, t) \quad \text{nematic alignment tensor} \tag{30}$$

$$\text{etc.} \tag{31}$$

We can obtain equations for these moments by integrating Eq. (27) over angles, with the result (for $d = 2$)

$$\partial_t \rho = -\boldsymbol{\nabla} \cdot (v_0 \mathbf{p}) \tag{32}$$

$$\partial_t \mathbf{p} = -D_r \mathbf{p} - \frac{1}{2} \boldsymbol{\nabla}(v_0 \rho) - \boldsymbol{\nabla} \cdot v_0 \mathbf{Q} \tag{33}$$

$$\partial_t \mathbf{Q} = -D_r \mathbf{Q} - \boldsymbol{\nabla}(...) \tag{34}$$

Each moment equation couples to higher order moments. To obtain a closed set of equations we neglect $\mathbf{Q}$ and higher moments and assume that for $t \gg D_R^{-1}$ the polarization density can be slaved to the conserved density, i.e., $\mathbf{p} \simeq -\frac{1}{2D_r} \boldsymbol{\nabla}(v_0 \rho)$. Substituting in Eq. (32), we obtain

$$\partial_t \rho = \boldsymbol{\nabla} \cdot \left(\frac{v_0}{2D_R} \boldsymbol{\nabla}(v_0 \rho) \right) = \frac{v_0^2}{2D_R} \nabla^2 \rho \,. \tag{35}$$

Clearly this is just the diffusion equation with diffusion coefficient $D_{sp} = v_0^2/(2D_R)$. It predicts that any fluctuation of the density from its homogeneous equilibrium value $\delta\rho = \rho - \rho_0$ decays in time, with $\delta\rho_{\mathbf{q}}(t) \sim e^{-D_{sp}q^2 t}$ for the decay of the corresponding Fourier amplitude.

As we argued earlier, interactions renormalize v_0 to a $v(\rho) < v_0$. Our MFT is obtained by replacing v_0 in Eq. (35) with $v(\rho)$, with the result

$$\partial_t \rho = \boldsymbol{\nabla} \cdot \mathcal{D}(\rho) \boldsymbol{\nabla} \rho \tag{36}$$

where

$$\mathcal{D}(\rho) = \frac{v(\rho)}{2D_r} \left[v(\rho) + \rho v'(\rho) \right] \tag{37}$$

and the prime denotes a derivative wrt ρ. If $v(\rho)$ is a sufficiently strongly decreasing function of ρ, then one can have $\mathcal{D}(\rho) < 0$ and density fluctuations will grow in time signaling, as we will see below, spinodal decomposition and phase separation. Explicit perturbative calculations give, to leading order in the density, $v(\rho) = v_0(1 - \tau_c/\tau_{mf}$, where τ_c is the mean duration of a collision and τ_{mf} the mean free time between collisions [10].

Equation(36) can be derived by explicit coarse graining of the microscopic dynamics. Here we will, however, follow a more generic approach based on field theory ideas and will discuss the implications of the equations in that context. Before doing this, it is useful to review the equilibrium description of phase separation in the context of the so-called Cahn-Hilliard equation or Model B.

Problem 3: Run-and-Tumble in $1D$.
Consider N particles undergoing run-and-tumble dynamics in one dimensions. These particles tumble at a constant rate α, but their run speed $v(x)$ is spatially varying. Such a situation can be achieved experimentally using, for instance, photokinetic *E.coli* [see G. Frangipane *et al.*, Dynamic density shaping of photokinetic *E. coli*, eLife **7**:e36608 (2018)]. Denote by $R(x,t)$ and $L(x,t)$ the density of right-moving and left-moving particles at time t.

1. Write Smoluchowski equations for the time evolution of R and L.
2. Reformulate the dynamics in terms of the total particle density $\rho = R + L$ and their polarization $p = R - L$.
3. Show that the dynamics can be recast in the mean-field form given in Eqs. (36-37) and identify the expression for $\mathcal{D}$. Clearly state the approximations you need to make to obtain this form and discuss whether you think they may apply to the experiments of Frangipane *et al.*.
4. Find the steady state solution $\rho_{ss}(x)$ of the equation you obtained in item 3 and contrast it to the steady state solution in the case where $v = v_0$.

Problem 3 highlights the difference betweew diffusion and the spontanoeus aggregation that drives MIPS. In equilibrium density inhomogeneities decay via diffusion and the steady state is homogeneous, with $\rho =$ constant. The persistent dynamics of ABPs, in contract, traps particles when their nose points towards high density regions and builds up density inhomogeneities.

The statistical physics of repulsive ABPs has been studied extensively, with the goal of constructing an effective thermodynamics for this system, including defining the pressure of an active gas, an effective surface tension, effective chemical potential, etc. [46].

MIPS has been seen in countless numerical simulations, but has it been seen in experiments? Experimental active systems, living and not, ubiquitously show aggregation in clusters and at surfaces. But are these really examples of MIPS? In general the interpretation of experiments in active colloids is complicated by a variety of phoretic effects, as well as hydrodynamic interactions. Experiments in bacteria are also complicated by hydrodynamic interactions, as well as chemotaxis, quorum sensing and more. The condensation of protein in membrane-free organelles inside living cells and their nucleus is presumably mediated by a variety of chemical reactions. In all these cases one observes arrested (as opposed to bulk) phase separation with the formation of dynamical clusters of well defined mean size. Nonetheless ABPs and their cousin models have allowed us to make great strides in the undertsanding the statitical physics of collection of particles whose dynamics breaks TRS. In fact ABPs have sometimes been referred to as "the Ising model" of active matter.

There are various mechanisms that can arrest phase separation, resulting in the selection of patterns or finite-size clusters. A generic one which is important in biological settings is the breaking of number conservation, as arising from cell division and death. This is achieved for instance by adding a logistic growth term to our MFT of MIPS to obtain dynamics described by the equation

$$\partial_t \rho = \boldsymbol{\nabla} \cdot [\mathcal{D}(\rho) \boldsymbol{\nabla} \rho] + \alpha \rho \left(1 - \frac{\rho}{\rho_0}\right) - \kappa \nabla^4 \rho \,, \tag{38}$$

where ρ_0 is the fixed uniform density of the model and the term proportional to interfacial tension κ is added to ensure stability at short scales. This model, studied for instance in Ref. [47], yields regular lattices of high density spots and concentric high density rings in $2D$, and captures some of the patterns observed in certain bacteria and usually explained by invoking chemotaxis. Pattern formation arises because reproduction and stabilizing surface tension compete with the destabilizing negative diffusivity from crowding, selecting a length scale $\sim \sqrt{|\mathcal{D}(\rho_0)|/\alpha}$.

B. Mapping MIPS onto Cahn-Hilliard-type theory: Model B^+

The phase separation of two immiscible fluids is a common phenomenon in everyday life (just think of oil and vinegar) used for the engineering of a variety of soft material and with important implications in biology. Generally a binary fluid consists of two fluid of A and B molecules that can exist in a well mixed homogeneous state at high temperature and in a demixed state of coexisting A-rich and B-rich phases separated by a fluid-fluid interface at low temperature. In equilibrium the demixing requires interspecies attractive interactions. A related phenomenon is gas-liquid condensation, where condensation again requires attractive interactions.

1. Cahn-Hilliard theory of Phase Separation - a brief review

Phase separation and its kinetics in equilibrium are well described by what are known as Model B and the Cahn-Hilliard equation. There are excellent reviews of this (e.g., Ref. [48]) and I will not spend a lot of time on it, but it is useful to review a few basic notions.

The continuum theory is formulated in terms of a scalar concentration field ϕ that describes the local composition of the binary fluid mixture (hence proportional to the difference between

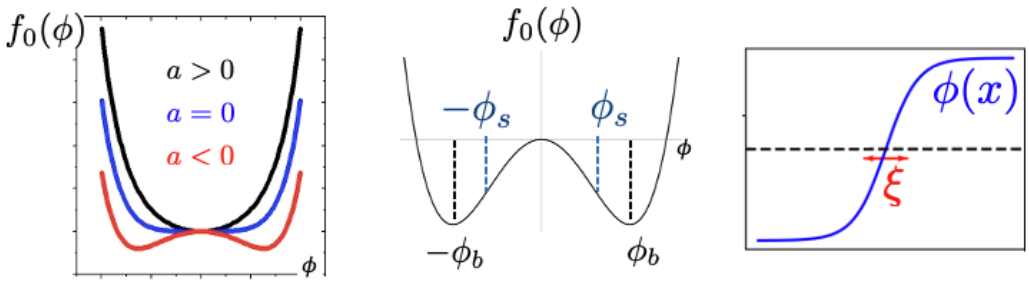

Figure 4. Left: the homogeneous free energy density f_0 is shown as a function of ϕ above ($a > 0$), at ($a = 0$) and below ($a < 0$) the transition. Center: The region $\phi_s \leq |\phi| \leq \phi_b$ is known as the binodal. In this region the homogeneous state is globally unstable, but locally stable, in the sense that a critical size fluctuation (critical nucleus) is required to initiate phase separation. The kinetics in the region proceed via nucleation and one must include noise for a description of the corresponding activated dynamics. The region $|\phi| < \phi_s$ is known as the spinodal region and is locally, as well as globally, unstable, i.e., any infinitesimal perturbation grows and destabilizes the homogeneous state. To describe the dynamics in this region we can neglect noise (but of course one must include some noise in the initial condition when simulating the dynamics). Right: the steady state profile of the interface.

concentration of A and of B molecules [1]) or the difference between the densities of the dense and dilute phases in the case of gas-liquid condensation. An approximate free energy for the system can then be written in the usual Landau fashion as an expansion in powers of the order parameter and its gradient. It can also be derived by coarse-graining. It is written as

$$F[\phi] = \int d\mathbf{r} \left[f_0(\phi) + \kappa (\nabla \phi)^2 \right] \ , \tag{39}$$

with

$$f_0(\phi) = \frac{a}{2}\phi^2 + \frac{b}{4}\phi^4 \ , \tag{40}$$

where $b > 0$ and a can change sign as a function of the parameter (say, temperature) that tunes the mixing-demixing transition. The homogeneous free energy $F_0 = V f_0$, with V the volume of the system, is the usual ϕ^4 energy used to model continuous phase transitions. For $a > 0$ it has a single minimum at $\phi = 0$. For $a < 0$ it has two minima at $\phi = -1$ (B-rich or dilute phase) and $\phi = +1$ (A-rich or dense phase). In other words, at $a = 0$ there is a transition from a homogeneous or well mixed state to a demixed or phase separated one (see Fig. 4). The energy scale κ is a stiffness and controls the surface tension $\sigma = (-8\kappa a^3/9b^2)^{1/2}$ and the thickness $\xi = (-\kappa/2a)^{1/2}$ of the interface.

The profile of the interface is easily obtained analytically by solving

$$\frac{\delta F}{\delta \phi} = a\phi + b\phi^3 - \kappa \nabla^2 \phi = 0 \tag{41}$$

---

[1] Here we consider the simplest case of a symmetric mixture where AA and BB interactions are the same.

with boundary conditions $\phi(\pm\infty) = \pm\phi_b$, with the result

$$\phi(x) = \phi_b \tanh\left(\frac{x}{\xi}\right) \ , \tag{42}$$

where we have chosen the midpoint of the interface at $x = 0$.

Note that Eq.(41) sets the exchange chemical potential

$$\mu_{eq} = \frac{\delta F}{\delta \phi} = a\phi + b\phi^3 - \kappa\nabla^2\phi \tag{43}$$

equal to zero. The exchange chemical potential is the difference in the chemical potentials of the two phases.

Problem 4:
Find the solution of Eq. (41) with the given boundary conditions.

The coarsening dynamics is described by an equation for the conserved field ϕ known as the Cahn-Hilliard equation, given by

$$\partial_t \phi = -\boldsymbol{\nabla} \cdot \mathbf{J}_\phi \ , \tag{44}$$

$$\mathbf{J}_\phi = -M\boldsymbol{\nabla}\mu_{eq} \ , \tag{45}$$

where M is the mobility. This is in general a nonlinear function of ϕ but here for simplicity it will be assumed to be constant, with $M = 1$. Explicitely, the Cahn-Hilliard equation is then given by

$$\partial_t \phi = \nabla^2\left(a\phi + \phi^3 - \kappa\nabla^2\phi\right) \tag{46}$$

where without loss of generality I have scaled ϕ to eliminate the coefficient of the ϕ^3 term. To examine the coarsening in the spinodal region, we linearize Eq. (46) about the homogeneous value ϕ_0 and examine the dynamics of the Fourier amplitudes of the fluctuations $\delta\phi = \phi - \phi_0 = \sum_{\mathbf{q}} \delta\phi_{\mathbf{q}}(t) e^{i\mathbf{q}\cdot\mathbf{r}}$, given by

$$\partial_t \delta\phi_{\mathbf{q}} = -q^2\left(D + \kappa q^2\right)\delta\phi_{\mathbf{q}} \ , \tag{47}$$

where $D = a + 3\phi_0^2$. Fluctuations decay/grow at the rate $r(q)$ according to $\delta\phi_{\mathbf{q}}(t) \sim e^{r(q)t}$. The dispersion relation $r(q)$ is shown in Fig. 5. For $D > 0$, $r(q) < 0$ and fluctuations decay diffusively. For $D < 0$, there is a band of wavenumbers where $r(q) > 0$ and fluctuations grow exponentially. Eventually nonlinearities kick in and stabilize a sharp interface. The system shows a bicontinuos structure and coarsens all the way to bulk phase separation. Late stage coarsening is driven by diffusive fluxes through a process called Ostwald ripening where small droplets shrink and large droplets grow. The scale $L(t)$ of the pattern is set by the wavenumber of the most unstable mode $L(t) \sim 1/q^*$. This grows in time with a characteristic exponent $L(t) \sim t^{1/3}$ and the pattern coarsens all the way to the system size. The $1/3$ growth law is easily understood by assuming that growth is controlled by a single length scale L moving at velocity v so that $\dot{L} \sim v$. If the dynamics of the system is dominated by diffusive currents, we estimate $v \sim \nabla\mu_{eq} \sim M\sigma/L^2$, where σ is the interfacial tension and I have restored the mobility M for clarity. Then $\dot{L} \sim M\sigma/L^2$, which gives $L(t) \sim t^{1/3}$.

In equilibrium the change of sign of a is controlled by the interplay of interaction energy versus entropy of mixing, the ϕ^4 term saturates the pattern amplitude, and the κ term cuts off the instability at short scales.

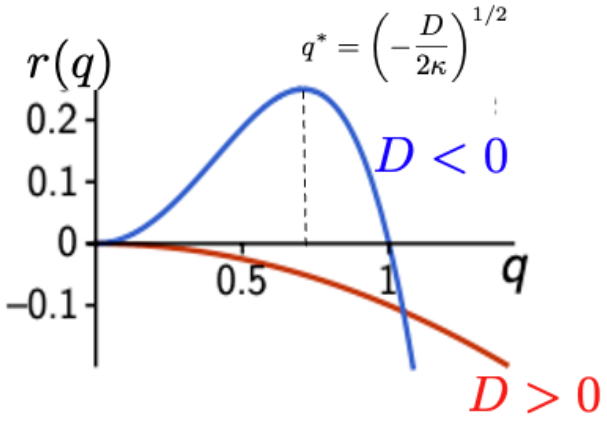

Figure 5. The dispersion relation obatined by lienarized the Cahn-Hilliard equation about a homogeneous state. For $D > 0$ the homogeneous state is stable and fluctuations decay diffusively (red curve). For $D < 0$ the homogeneous state is unstable and fluctuations grow exponentially in a band of wavnumber. The dispersion relation has the characteristic spinodal shape. The wavenumber q^* describes the fastest growing modes.

2. A field theory for MIPS

One can constructt a field theory of MIPS by mapping the dynamics onto a Cahn-Hilliard-type model [49, 50]. In this mapping the scalar field ϕ is proportional to the difference between the densities of the dense and dilute phases. The MFT introduced earlier would give a coventional CH model, where the change of sign of a is controlled by the slowing down of motile particles upon crowding. It has in fact been shown that the effect of motility suppression due to crowding can be mapped onto an effective attractive interaction. The lack of detailed balance in collections of ABPs, however, allows for new terms that are forbidden in equilibrium. The current takes the form [50, 51]

$$\mathbf{J} = -\boldsymbol{\nabla}\mu_{eq} - \lambda\boldsymbol{\nabla}(\boldsymbol{\nabla}\phi)^2 + \zeta(\nabla^2\phi)\boldsymbol{\nabla}\phi \tag{48}$$

When combined with the continuity equation for the ϕ field, Eq. (48) gives what is known as Model B^+. The first term on the right hand side is simply the gradient of the chemical potential obtained as a gradient of the free energy. This term alone preserves TRS and provides the MF description of MIPS given in the previous section. When only this term is retained, one finds that ABPs always coarsen to complete (bulk) phase separation. The other two terms, proportional to λ and ζ, break TRS and cannot be written as derivatives of a free energy. Both these TRS-breaking terms have little effect on the spinodal instability as they do not contribute to linear order. Additionally, the λ term has only a quantitative effect on the phase diagram by shifting the spinodal line to the right or left depending on the sign of λ. The ζ term, however, has qualitative new effects as it can arrest the coarsening via a process dubbed reverse Ostwald ripening, resulting in microphase separation [51]. For more details on these field theories I refer you to the work by the group of Mike Cates and to a review, Ref. [50]. The precise microscopic origin of this terms remains an open question.

C. Nonreciprocal Phase Separation

Multispecies systems with effective cross-interactions that are non-reciprocal, that is evade Newton's third law of action-reaction, have received a lot of interest in recent years [5, 52, 53]. At the microscale, nonreciprocity is intrinsically rooted in the breaking of detailed balance. At a mesoscopic scale, it manifests itself in effective dynamical cross couplings that correspond to non-conservative forces and cannot be obtained as derivatives of a Hamiltonian or free energy. Such non-reciprocity is ubiquitous in active and nonequilibrium systems [54]. It occurs, for instance, in predator-prey systems [55], active solids with odd elasticity [56], protein-based pattern formation [57], mixtures of active and passive particles [52, 58], directional interface growth [59], and non-Hermitian quantum systems [60]. Such systems can spontaneously organize in dynamical steady states with nontrivial temporal order, such as traveling and oscillating states.

In the context of our discussion, a minimal system that highlights the consequences of NR interactions is a mixture of active and passive Brownian particles. The active particles can undergo MIPS, and in MF their dynamics can be described by a Cahn-Hilliard-type equation. The passive particles are simply diffusive. The two are additionally coupled by cross-diffusivities. If we denote by ρ_A and ρ_P the conserved densities of active and passive particles, their coupled dynamics can be described by the following set of equations [61]

$$\partial_t \rho_A(x,t) = \nabla^2 (D_{AA}\rho_A + \rho_A^3 - \kappa \nabla^2 \rho_A + D_{AP}\rho_P) \,, \tag{49}$$

$$\partial_t \rho_P(x,t) = \nabla^2 (D_{PP}\rho_P + D_{PA}\rho_A) \,. \tag{50}$$

These equations can be derived by coarse-graining the microscopic dynamics [52, 58]. In general, all the diffusivities D_{ab} are found to be nonlinear functions of the densities. For simplicity, here we will assume them constant. Since these fields are conserved, the dynamics of fluctuations is controlled by soft or hydrodynamic modes, defined as those where a fluctuation of wavenumber q decays (or grows) at a rate $\sigma(q)$, with $\lim_{q\to 0} \Re[\sigma(q)] = 0$. In the absence of cross couplings, fluctuations in ρ_P decay diffusively, while D_{AA} can become negative in a range of densities and Péclet numbers as the persistent dynamics of ABPs drives MIPS. Therefore fluctuations in ρ_A exhibit the characteristic dispersion relation of a spinodal instability, with largest growth at a characteristic length scale controlled by $|D_{AA}|$ and κ. Cross-diffusion couples the two hydrodynamic modes, but the dispersion relation branches do not cross for cross diffusivities that are equal or obey Onsager's rules (Fig. 6(a)). On the other hand, active particles are slowed down by both other active particles, as well as by passive particles. For this reason, the cross diffusivity D_{AP} can also be negative in a range of densities. Passive Brownian particles, in contrast, undergo conventional diffusions, hence D_{PP}, $D_{PA} > 0$. There is therefore a regime of parameters where the two density fields are coupled not just non-reciprocally, but antagonistically, i.e., $D_{AP} < 0$, $D_{PA} > 0$. One can show that nonreciprocal cross-diffusivities cause the two modes to cross, where the two eigenvectors align at the crossing point, resulting in the appearance of an imaginary part of the dispersion relation [green dashed lines in Fig. 6(a)]. In other words, nonreciprocal couplings lead to mode coalescence and transform the static phase separated state into traveling [Fig. 6(c)] or oscillating domains [52, 53].

Again here a linear stability analysis of the homogeneous state provides much insight. If we linearize the equations about a global steady state, $(\rho_A, \rho_P) = (\rho_A^0, \rho_P^0)$, for perturbations of the form $e^{iqx+\sigma t}$ we find that the modes governing the time evolution of fluctuations are the eigenvalues of the Jacobian

$$J = q^2 \begin{pmatrix} -D_{AA} - 3(\rho_A^0)^2 - \kappa q^2 & -D_{AP} \\ -D_{PA} & -D_{PP} \end{pmatrix} \tag{51}$$

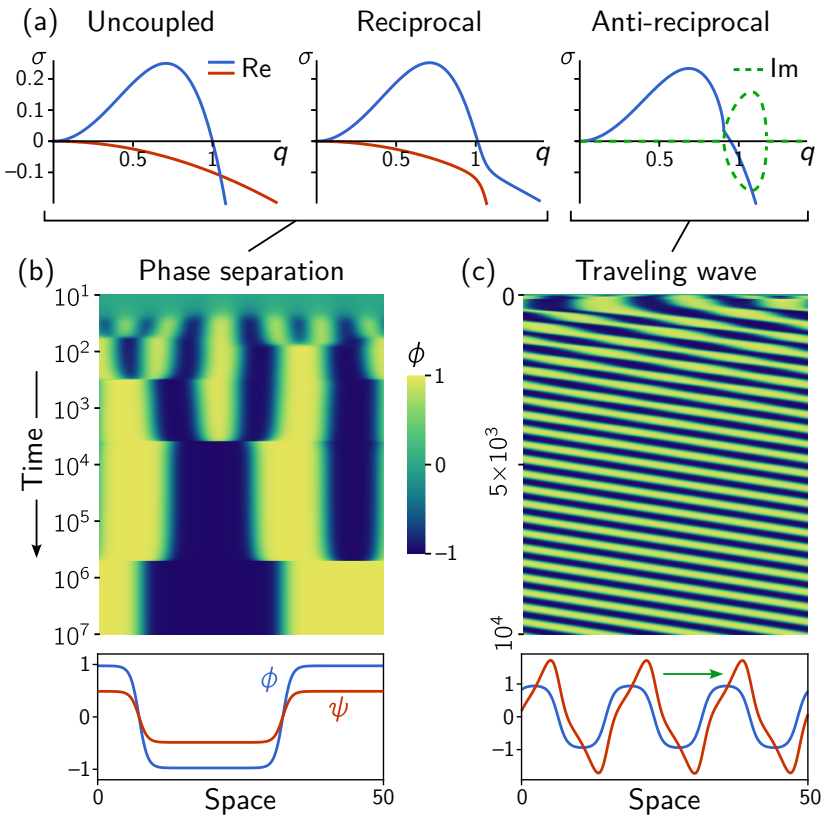

Figure 6. (a) Dispersion relations for the cases $D_{AP} = D_{PA} = 0$ (left), $D_{AP}D_{PA} > 0$ (center) and $D_{AP}D_{PA} < 0$ (right). (b) A kymograph showing the coarsening of the two densities all the way to bulk phase separation for reciprocal couplings. Here $\phi \equiv \rho_A$ and $\psi \equiv \rho_P$. (c) A kymograph showing the arrested coarsening of the two densities and onset of traveling waves for non reciprocal couplings.

In the uncoupled case ($D_{AP}D_{PA} = 0$), the dispersion relation has two independent branches given by the diagonal entries in the Jacobian [see Fig. 6(a), left frame]. A band of unstable modes $[0, q_+]$ emerges in the first branch when $D_{AA} < -3(\rho_A^0)^2$, where $q_+^2 = (-D_{AA} - 3(\rho_A^0)^2)/\kappa$. This is the spinodal decomposition instability that drives phase separation. Cross-diffusive couplings cause the branches of the dispersion relation to interact near their intersection point, giving rise to a band of propagating modes ($\mathrm{Im}[\sigma] \neq 0$) in the anti-reciprocal case $D_{AP}D_{PA} < 0$; see Fig. 6(a), right frame. For sufficiently strong anti-reciprocal coupling, the band of propagating modes begins to overlap with the band of unstable modes $[0, q_+]$. For $D_{AP}D_{PA} = -D_{PP}^2$, the marginal mode q_+ touches the band of propagating modes. At this point, the Jacobian has two vanishing eigenvalues and is non-diagonalizable, i.e., its eigenvectors coincide. This marks an "exceptional point" [54, 60].

On the basis of the linear stability analysis one can construct a phase diagram (see Fig. 7) that reproduces well the reuslt of numerical integration of the equations.

Note that the traveling waves break both TRS and parity ($\mathbf{r} \to -\mathbf{r}$). Hence this is referred to as a PT-breaking transition.

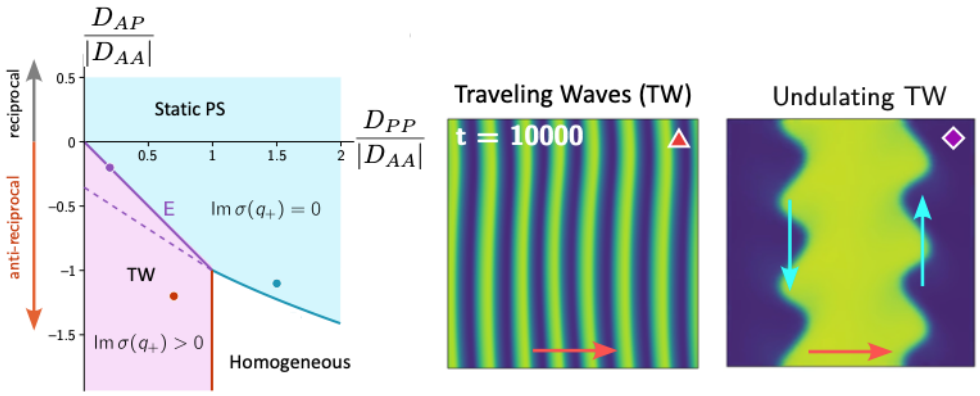

Figure 7. Left: Linear stability diagram in the D_{PP}-D_{AP} parameter plane where we set $D_{AP} = |D_{PA}|$, such that the sign of D_{AP} determines whether the coupling is reciprocal ($D_{AP} > 0$) or anti-reciprocal ($D_{AP} < 0$). Along the purple line (E) an "exceptional point" appears in the dispersion relation, where the band of unstable modes touches the band of propagating modes. When the diffusion of ρ_P is fast (large D_{PP}) pattern formation is suppressed and the homogeneous well mixed state is again stable. Middle: traveling waves (TW) in $2D$. Right: undulating traveling waves in $2D$.

There are two new findings here. First, while TW and oacillations are ubiquitous and well understood in nonlinearly dynamical systems with activator/inhibitor couplings through models with with few degrees of freedom (e.g. FitzHugh–Nagumo equations [62, 63]) they are unexpected in purely diffusive systems and generally less explored in spatially extended systems. On the other hand, the appearance of TW may not be so suprising as it is the result of the antagonistic cross-diffusivities: active particles are effectively attracted to passive ones, but passives one are repelled by active ones through steric effects. This leads to a chase-and-run dynamics where the two fields eventually settle into a state where they travel at a relative constant velocity. More suprising, however, is that one also gets patterns (not just bulk phase separation) of well-defined wavelength. This is suprising becasue the model itself only contains one length scale (the interface width). The mechanisms for wavelength selection are still under investigation [61]. There are also secondary instabilities, such as traveling undulations that travel along stripes, that are very intriguing.

A similar mechanism is at play in the antagonistic coupling of two groups of flocking agents described for instance by non-reciprocally coupled Toner-Tu equations [54]. In the absence of coupling, each population undergoes a phase transition to a state of finite mean motion that spontaneously breaks polar symmetry [15] - the nonequilibrium analog of a finite magnetization in interacting XY spins. When the two populations A and B are coupled antireciprocally (A wants to align with B, but B wants to antialign with A) the system is dynamically frustrated and organizes into a state of chase-and-run motion, where birds chase each other tails, that breaks chiral symmetry [54]. Both sets of results have opened up a flurry of activity on the role of non-reciprocity in dynamical pattern formation [5] and the search for generic models of nonequilibrium transitions from static to time-ordered states [64].

There are two additional important points to be made. First, the structure of the linear fluctuation spectrum seen in the NRCH model (merging of the real part of the two hydrodynamic modes and simultaneous emergence of a finite imaginary part, associated with the non-diagonalizable form of the matrix that governs the linear dynamics of fluctuations and degenerate eigenvectors → ex-

ceptional point) is a distinct signature of temporal organization, hence provides a criterion for identifying a new class of dynamical pattern formation (see also [64]). This mechanism is analogue to the one responsible for the onset of chiral states in antagonistic flocking models [54]. There is, however, a difference between the two systems. In NRCH the hydrodynamic nature of the fluctuations guarantees that for strong enough nonreciprocity the merging will occur for all parameter values, hence it is generic. In flocking models the velocity order parameter is not conserved. Instead, the spontaneously broken rotational symmetry of the flocking state is associated with the emergence of a Goldstone mode with relaxation rate that vanishes at long wavelength. The mode coalescence therefore happens *globally* instead of *locally*.

Second, there are a number of experimental systems where TW and oscillations have been observed that can all be recast in the NRCH framework. In addition to the active/passive particles mixture discussed earlier, other examples are mass-conserving reaction-diffusion systems, viscoelastic gels and active interfaces [61].

Open-ended Problem:
A very recent press release by Ramin Golestanian in Europhysics News hihglights the rapidly growing interest in nonreciprocal interaction in non-equilibrium systems (`https://www.europhysicsnews.org/articles/epn/pdf/2024/03/epn2024553p12.pdf`).

Research the literature to identify an experimental system where traveling and/or oscillating states are observed and the dynamics can be mapped onto the NRCH model. Address the following questions:

(i) Which are the coupled hydrodynamic fields at play in the system of your choice?

(ii) Why are they "hydrodynamics" (conserved fields, Goldstone modes, other)?

(iii) What are the physical mechanisms that engender effective NR interactions?

(iv) What are the experimental observation?

(v) Do you think the system you have identified is a promising candidate for observing some of the predictions of NRCH models? What would you measure to establish the connection?

---

[1] Sriram Ramaswamy, "The mechanics and statistics of active matter," Annu. Rev. Condens. Matter Phys. **1**, 323–345 (2010).

[2] M Cristina Marchetti, Jean-François Joanny, Sriram Ramaswamy, Tanniemola B Liverpool, Jacques Prost, Madan Rao, and R Aditi Simha, "Hydrodynamics of soft active matter," Reviews of Modern Physics **85**, 1143 (2013).

[3] Clemens Bechinger, Roberto Di Leonardo, Hartmut Löwen, Charles Reichhardt, Giorgio Volpe, and Giovanni Volpe, "Active particles in complex and crowded environments," Rev. Mod. Phys. **88**, 045006 (2016).

[4] Daniel Needleman and Zvonimir Dogic, "Active matter at the interface between materials science and cell biology," Nature Reviews Materials **2**, 1–14 (2017).

[5] Mark J Bowick, Nikta Fakhri, M Cristina Marchetti, and Sriram Ramaswamy, "Symmetry, thermodynamics, and topology in active matter," Physical Review X **12**, 010501 (2022).

[6] Suraj Shankar, Anton Souslov, Mark J Bowick, M Cristina Marchetti, and Vincenzo Vitelli, "Topological active matter," Nature Reviews Physics **4**, 380–398 (2022).

[7] Michael te Vrugt and Raphael Wittkowski, "A review of active matter reviews," arXiv e-prints , arXiv–2405 (2024).

[8] Michael E Cates, "Diffusive transport without detailed balance in motile bacteria: does microbiology need statistical physics?" Reports on Progress in Physics **75**, 042601 (2012).

[9] Howard C Berg, *Random walks in biology* (Princeton University Press, 1993).

[10] M Cristina Marchetti, Yaouen Fily, Silke Henkes, Adam Patch, and David Yllanes, "Minimal model of active colloids highlights the role of mechanical interactions in controlling the emergent behavior of active matter," Current Opinion in Colloid & Interface Science **21**, 34–43 (2016).
[11] Antoine Bricard, Jean-Baptiste Caussin, Nicolas Desreumaux, Olivier Dauchot, and Denis Bartolo, "Emergence of macroscopic directed motion in populations of motile colloids," Nature **503**, 95–98 (2013).
[12] Tim Sanchez, Daniel TN Chen, Stephen J DeCamp, Michael Heymann, and Zvonimir Dogic, "Spontaneous motion in hierarchically assembled active matter," Nature **491**, 431 (2012).
[13] Vishal Soni, Ephraim S Bililign, Sofia Magkiriadou, Stefano Sacanna, Denis Bartolo, Michael J Shelley, and William TM Irvine, "The odd free surface flows of a colloidal chiral fluid," Nature Physics **15**, 1188–1194 (2019).
[14] Tamás Vicsek, András Czirók, Eshel Ben-Jacob, Inon Cohen, and Ofer Shochet, "Novel type of phase transition in a system of self-driven particles," Physical Review Letters **75**, 1226 (1995).
[15] John Toner and Yuhai Tu, "Long-range order in a two-dimensional dynamical xy model: how birds fly together," Physical Review Letters **75**, 4326 (1995).
[16] Craig W Reynolds, "Flocks, herds and schools: A distributed behavioral model," in *Proceedings of the 14th annual conference on Computer graphics and interactive techniques* (1987) pp. 25–34.
[17] Ichiro Aoki, "A simulation study on the schooling mechanism in fish." NIPPON SUISAN GAKKAISHI (Bulletin of the Japanese Society of Scientific Fisheries) **48**, 1081–1088 (1982).
[18] Brian L Partridge, "The structure and function of fish schools," Scientific American **246**, 114–123 (1982).
[19] Sriram Ramaswamy and R Aditi Simha, "The mechanics of active matter: Broken-symmetry hydrodynamics of motile particles and granular layers," Solid state communications **139**, 617–622 (2006).
[20] J Prost and R Bruinsma, "Shape fluctuations of active membranes," EPL (Europhysics Letters) **33**, 321 (1996).
[21] Sriram Ramaswamy, John Toner, and Jacques Prost, "Nonequilibrium fluctuations, traveling waves, and instabilities in active membranes," Physical review letters **84**, 3494 (2000).
[22] James Darnell, Harvey Lodish, and David Baltimore, *Molecular cell biology.*, QH581. 2 D22 1990 (1990).
[23] BA Finlayson and LE Scriven, "Convective instability by active stress," Proceedings of the Royal Society of London. A. Mathematical and Physical Sciences **310**, 183–219 (1969).
[24] Robert Zwanzig, *Nonequilibrium statistical mechanics* (Oxford university press, 2001).
[25] Yaouen Fily and M Cristina Marchetti, "Athermal phase separation of self-propelled particles with no alignment," Physical review letters **108**, 235702 (2012).
[26] Gabriel S Redner, Michael F Hagan, and Aparna Baskaran, "Structure and dynamics of a phase-separating active colloidal fluid," Biophysical Journal **104**, 640a (2013).
[27] Mark J Schnitzer, "Theory of continuum random walks and application to chemotaxis," Physical Review E **48**, 2553 (1993).
[28] Julien Tailleur and Michael E Cates, "Statistical mechanics of interacting run-and-tumble bacteria," Physical review letters **100**, 218103 (2008).
[29] Claudio Maggi, Umberto Marini Bettolo Marconi, Nicoletta Gnan, and Roberto Di Leonardo, "Multidimensional stationary probability distribution for interacting active particles," Scientific reports **5**, 10742 (2015).
[30] Thomas FF Farage, Philip Krinninger, and Joseph M Brader, "Effective interactions in active brownian suspensions," Physical Review E **91**, 042310 (2015).
[31] C. Nardini, É Fodor, E. Tjhung, F. van Wijland, J. Taileur, and M. E. Cates, "Entropy production in field theoreis without time-reversal symmetry: quantifying the non-equilibrium character of active matter," Phys. Rev. X **7**, 021007 (2017).
[32] R. Aditi Simha and Sriram Ramaswamy, "Hydrodynamic fluctuations and instabilities in ordered suspensions of self-propelled particles," Phys. Rev. Lett. **89**, 058101 (2002).
[33] Paul C Martin, Olivier Parodi, and Peter S Pershan, "Unified hydrodynamic theory for crystals, liquid crystals, and normal fluids," Physical Review A **6**, 2401 (1972).

[34] Karsten Kruse, Jean-François Joanny, Frank Jülicher, Jacques Prost, and Ken Sekimoto, "Asters, vortices, and rotating spirals in active gels of polar filaments," Physical review letters **92**, 078101 (2004).
[35] Eric Bertin, Michel Droz, and Guillaume Grégoire, "Boltzmann and hydrodynamic description for self-propelled particles," Physical Review E—Statistical, Nonlinear, and Soft Matter Physics **74**, 022101 (2006).
[36] Anton Peshkov, Eric Bertin, Francesco Ginelli, and Hugues Chaté, "Boltzmann-ginzburg-landau approach for continuous descriptions of generic vicsek-like models," The European Physical Journal Special Topics **223**, 1315–1344 (2014).
[37] David S Dean, "Langevin equation for the density of a system of interacting langevin processes," Journal of Physics A: Mathematical and General **29**, L613 (1996).
[38] Jonathan Colen, Ming Han, Rui Zhang, Steven A Redford, Linnea M Lemma, Link Morgan, Paul V Ruijgrok, Raymond Adkins, Zev Bryant, Zvonimir Dogic, *et al.*, "Machine learning active-nematic hydrodynamics," Proceedings of the National Academy of Sciences **118** (2021).
[39] Rohit Supekar, Boya Song, Alasdair Hastewell, Gary PT Choi, Alexander Mietke, and Jörn Dunkel, "Learning hydrodynamic equations for active matter from particle simulations and experiments," Proceedings of the National Academy of Sciences **120**, e2206994120 (2023).
[40] Michael E Cates and Julien Tailleur, "Motility-induced phase separation," Annu. Rev. Condens. Matter Phys. **6**, 219–244 (2015).
[41] Silke Henkes, Yaouen Fily, and M Cristina Marchetti, "Active jamming: Self-propelled soft particles at high density," Physical Review E—Statistical, Nonlinear, and Soft Matter Physics **84**, 040301 (2011).
[42] Liesbeth MC Janssen, "Active glasses," Journal of Physics: Condensed Matter **31**, 503002 (2019).
[43] Dapeng Bi, Xingbo Yang, M Cristina Marchetti, and M Lisa Manning, "Motility-driven glass and jamming transitions in biological tissues," Physical Review X **6**, 021011 (2016).
[44] Elizabeth Lawson-Keister and M Lisa Manning, "Jamming and arrest of cell motion in biological tissues," Current Opinion in Cell Biology **72**, 146–155 (2021).
[45] Pasquale Digregorio, Demian Levis, Antonio Suma, Leticia F Cugliandolo, Giuseppe Gonnella, and Ignacio Pagonabarraga, "Full phase diagram of active brownian disks: from melting to motility-induced phase separation," Physical review letters **121**, 098003 (2018).
[46] Ydan Ben Dor, Yariv Kafri, and Julien Tailleur, "Forces in dry active matter," arXiv preprint arXiv:1811.08829 (2018).
[47] Michael E Cates, D Marenduzzo, I Pagonabarraga, and J Tailleur, "Arrested phase separation in reproducing bacteria creates a generic route to pattern formation," Proceedings of the National Academy of Sciences **107**, 11715–11720 (2010).
[48] Michael E Cates and Elsen Tjhung, "Theories of binary fluid mixtures: from phase-separation kinetics to active emulsions," Journal of Fluid Mechanics **836**, P1 (2018).
[49] Joakim Stenhammar, Adriano Tiribocchi, Rosalind J Allen, Davide Marenduzzo, and Michael E Cates, "Continuum theory of phase separation kinetics for active brownian particles," Physical review letters **111**, 145702 (2013).
[50] MICHAEL E Cates, "Active field theories," Active matter and nonequilibrium statistical physics: lecture notes of the Les Houches summer school 2018 , 180–216 (2022).
[51] Elsen Tjhung, Cesare Nardini, and Michael E Cates, "Cluster phases and bubbly phase separation in active fluids: reversal of the ostwald process," Physical Review X **8**, 031080 (2018).
[52] Zhihong You, Aparna Baskaran, and M Cristina Marchetti, "Nonreciprocity as a generic route to traveling states," Proceedings of the National Academy of Sciences **117**, 19767–19772 (2020).
[53] Suropriya Saha, Jaime Agudo-Canalejo, and Ramin Golestanian, "Scalar active mixtures: The nonreciprocal cahn-hilliard model," Physical Review X **10**, 041009 (2020).
[54] Michel Fruchart, Ryo Hanai, Peter B Littlewood, and Vincenzo Vitelli, "Non-reciprocal phase transitions," Nature **592**, 363–369 (2021).
[55] Tobias Reichenbach, Mauro Mobilia, and Erwin Frey, "Mobility promotes and jeopardizes biodiversity in rock–paper–scissors games," Nature **448**, 1046–1049 (2007).
[56] Colin Scheibner, Anton Souslov, Debarghya Banerjee, Piotr Surówka, William T. M. Irvine, and Vincenzo Vitelli, "Odd elasticity," Nature Physics **16**, 475–480 (2020).

[57] Jacob Halatek, Fridtjof Brauns, and Erwin Frey, "Self-organization principles of intracellular pattern formation," Philosophical Transactions of the Royal Society B: Biological Sciences **373**, 20170107 (2018).
[58] Raphael Wittkowski, Adriano Tiribocchi, Joakim Stenhammar, Rosalind J. Allen, Davide Marenduzzo, and Michael E. Cates, "Scalar Φ4 field theory for active-particle phase separation," Nature Communications **5**, 4351 (2014).
[59] Lihong Pan and John R. de Bruyn, "Nonuniform broken-parity waves and the Eckhaus instability," Physical Review E **49**, 2119–2129 (1994).
[60] Mohammad-Ali Miri and Andrea Alù, "Exceptional points in optics and photonics," Science **363**, eaar7709 (2019).
[61] Fridtjof Brauns and M Cristina Marchetti, "Nonreciprocal pattern formation of conserved fields," Physical Review X **14**, 021014 (2024).
[62] Richard FitzHugh, "Impulses and Physiological States in Theoretical Models of Nerve Membrane," Biophysical Journal **1**, 445–466 (1961).
[63] J. Nagumo, S. Arimoto, and S. Yoshizawa, "An Active Pulse Transmission Line Simulating Nerve Axon," Proceedings of the IRE **50**, 2061–2070 (1962).
[64] Tobias Frohoff-Hülsmann and Uwe Thiele, "Nonreciprocal Cahn-Hilliard Model Emerges as a Universal Amplitude Equation," Physical Review Letters **131**, 107201 (2023).